Development of an LS-DYNA Model of an ATR42-300 Aircraft for Crash Simulation

Karen E. Jackson and Edwin L. Fasanella

U.S. Army Research Laboratory, Vehicle Technology Directorate, Hampton VA

Abstract

This paper describes the development of an LS-DYNA simulation of a vertical drop test of an ATR42-300 twin-turboprop high-wing commuter-class airplane. A 30-ft/s drop test of this aircraft was performed onto a concrete impact surface at the FAA Technical Center on July 30, 2003. The purpose of the test was to evaluate the structural response of a commuter category aircraft when subjected to a severe, but survivable, impact. The aircraft was configured with crew and passenger seats, anthropomorphic test dummies, forward and aft luggage, instrumentation, and other ballast. The wings were filled with approximately 8,700 lb. of water to represent the fuel and the aircraft weighed a total of 33,200 lb. The model, which consisted of 57,643 nodes and 62,979 elements, was developed from direct measurements of the airframe geometry. The seats, dummies, luggage, fuel, and other ballast were represented using concentrated masses. Comparisons were made of the structural deformation and failure behavior of the airframe, as well as selected acceleration time history responses.

Introduction

This paper describes the development and validation of a full-scale finite element model of an ATR42-300 commuter-class aircraft for crash simulation. The model was developed prior to the test and analytical predictions were generated for correlation with the experimental data. Model validations, such as described in this paper, are necessary to gain confidence in the application of explicit transient dynamic finite element codes for crashworthy design and certification. In fact, the "validation of numerical simulations" was identified as one of five key technology shortfalls during the Workshop on Computational Methods for Crashworthiness that was held at NASA Langley Research Center in 1992 [1].

In 1998, the U.S. Army Research Laboratory Vehicle Technology Directorate (ARL-VTD) entered into an Inter-Agency Agreement (IAA) with the Federal Aviation Administration (FAA) William J. Hughes Technical Center for the purpose of validating crash simulations of airframe structures. As part of the IAA, finite element models were constructed of two 10-ft. long Boeing 737 (B737) fuselage sections, one outfitted with an auxiliary fuel tank mounted beneath the floor and the other with two different overhead stowage bins and luggage. Vertical drop tests of these two fuselage sections were performed at the FAA Technical Center in 1999 and 2000, respectively [2, 3]. These tests provided a valuable opportunity to evaluate the capabilities of computational tools for crash simulation through analytical/experimental correlation. Full-scale three-dimensional finite element models of the B737 fuselage sections were developed using MSC.Dytran [4], a commercial explicit transient dynamic code, and simulations of the vertical drop tests were executed. The analytical predictions were successfully validated through extensive test-analysis correlation, as documented in References 5 through 7.

In 2003, the IAA was extended for an additional five years (through 2008) and the model validation work entered a new phase with the development of a full-scale finite element model of the ATR42-300 aircraft. For this simulation, the model was developed using the pre-processing software package, MSC.Patran [8], and the final model was executed using another commercial

code, LS-DYNA [9]. The FAA performed a 30-ft/s vertical drop test of the aircraft to determine the impact responses of the airframe, floor, seat tracks, seats, Anthropomorphic Test Dummies (ATDs), and high-wing fuel system. Recently, the FAA has proposed dynamic performance criteria for seats in commuter aircraft that were based on empirical information obtained from prior airplane crash test data, which did not include airplanes representative in size of commuters. Consequently, this experiment was performed to provide impact data to evaluate the seat standards for this category of aircraft. The experimental program, model development process, and test-analysis correlations are presented in subsequent sections of the paper.

Experimental Program

On July 30, 2003, a 30-ft/s vertical drop test of an ATR42 aircraft was conducted using the Dynamic Drop Test Facility located at the FAA Technical Center. A pre-test photograph of the test article, raised to the drop height of 14-ft., is shown in Figure 1. This twin-turboprop, high-wing, commuter-class aircraft was developed and manufactured through a joint effort by Aerospatiale in France and Aeritalia in Italy. The aircraft has a wingspan of 80 ft., a seating capacity of 42-50 passengers, a maximum cruise speed of 304 knots/hour, and a maximum gross take-off weight of approximately 36,800 lb. The drop test was performed onto a concrete surface. The purpose of the test was to evaluate the dynamic structural response of the aircraft when subjected to a severe, but survivable, impact. Particular attention was given to the seat and occupant responses to evaluate the FAA's proposed dynamic seat requirements for commuter-class aircraft.

A schematic drawing of the floor of the aircraft is shown in Figure 2. The total weight of the aircraft prior to the drop test was 33,200 lb. A large portion of the total weight was the 8,700-lb. of water added to the fuel tanks in the wings to represent fuel. In addition, 16 double-occupant aircraft seats weighing 54 lb. each and 3 single-occupant seats weighing 20 lb. each were attached to seat tracks on the floor, as shown in Figure 2. Seven ATDs and 16 mannequins, each weighing approximately 170 lb., were seated in various locations, as indicated in Figure 2. Ballast weights equaling 135- and 152-lb. were added to some of the empty seats to represent the mass of occupants. The forward and aft storage compartments were filled with 1,450- and 739-lb. of luggage, respectively. In addition to the ballast, two overhead stowage bins were mounted between Frame Station 30 (FS 30) and FS 34 on the right and left sides of the fuselage. The bins weighed 55 lb. each (22-lb. empty weight plus 33-lb. ballast in each bin). Two concentrated masses were added to the engine mounts on the wings, each weighing 1, 290 lb., to represent the simulated engines.

A dominant feature of this aircraft is the high wing, which is attached directly to heavy fuselage frames at FS 25 and FS 27 through four "dog bone" specimens. The dog bone specimens attach to the fuselage frames at a location approximately 60 in. above the floor. Four additional attachments are located at the very top of the fuselage frames.

The measured longitudinal position of the center-of-gravity (CG) of the aircraft is approximately half way between FS 25 and FS 26, as shown in Figure 2. This measurement closely matches the CG location specified by the airframe manufacturer, as indicated in the Weight and Balance Manual [10].

Figure 1. Pre-test photograph of the ATR42 aircraft, raised to a drop height of 14 feet.

The fuselage section was instrumented with accelerometers, strain gages, load cells, pressure transducers, and string potentiometers. Test data were collected at 10,000 samples per second using two data acquisition systems, one on-board and one off-board. Of the channels available, eight acceleration responses were selected for correlation with the model. Of these eight responses, five were from accelerometers mounted on the floor of the fuselage cabin at locations shown in Figure 2. In addition, accelerometers located in the tail section at FS 47, the left sidewall at FS 18, and the center ceiling at FS 26 were also selected for comparison. These locations are not shown in Figure 2.

A post-test photograph showing an overall exterior view of the aircraft is shown in Figure 3. The dominant damage mode to the airframe was the failure of the heavy fuselage frames supporting the wing, causing the wing to subsequently displace through the fuselage cabin. The aluminum structure supporting the wing was crushed and fractured. A post-test photograph showing a closer view of the wing/fuselage region is shown in Figure 4(a). Further inspection of the airframe following the test indicated that several of the seats failed, as shown in Figure 4(b).
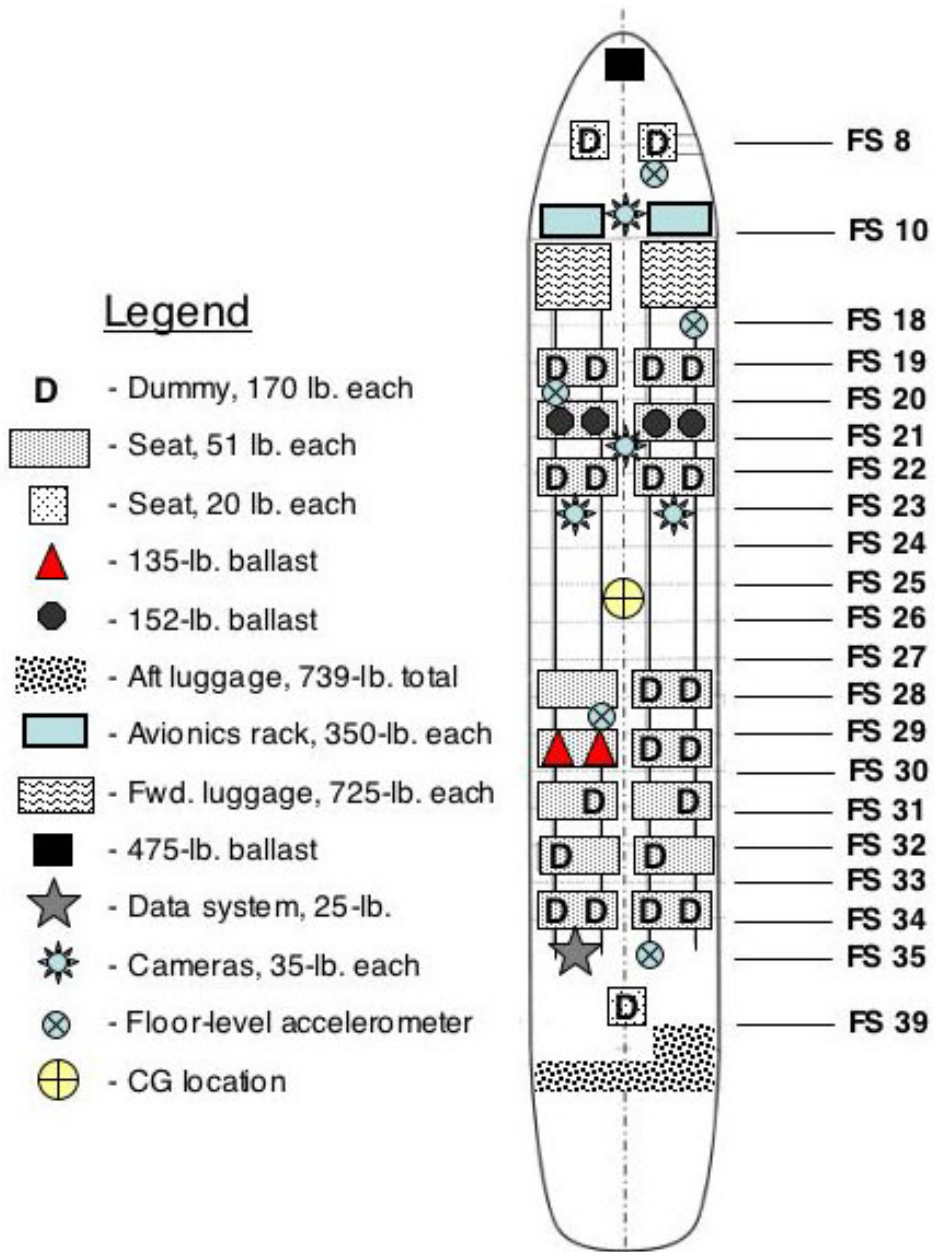
Figure 2. Floor schematic.

Figure 3. Post-test photograph of the ATR42 aircraft showing an overall view.

(a) Close-up view.   (b) Interior view.

Figure 4. Post-test photographs.

Model Development

The finite element model of the ATR42 aircraft was developed from geometric data gathered from direct measurements of the aircraft, which were input into MSC.Patran database files. The geometric data were received from the FAA in six installments, each containing increasingly more detailed information on the shape and dimensions of the airframe. As each file was received, the new information was input into a master geometry file of the entire aircraft. The final geometry model of the aircraft, shown in Figure 5, consisted of 25,917 points; 17,270 curves; and 17,768 surfaces. The geometry model was discretized into a finite element mesh, element and material properties were assigned, contact and initial velocity conditions were defined, and the model was executed to generate analytical predictions of structural deformation and acceleration time history responses.
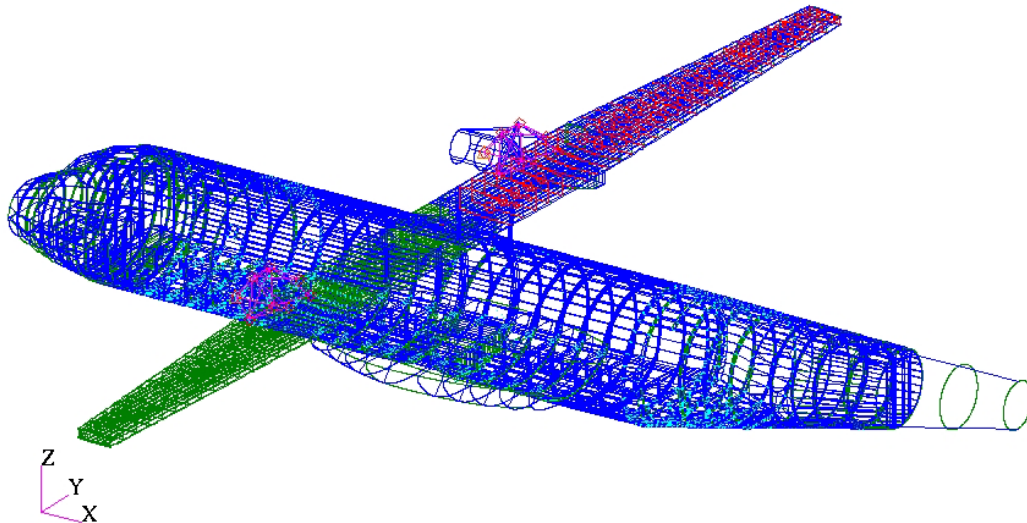
Figure 5. Final geometry model of the ATR42 aircraft.

The finite element model of the ATR42 aircraft, shown in Figure 6, contained 57,643 nodes and 62,979 elements including 60,197 quadrilateral shell elements; 551 triangular shell elements; 526 beam elements; and, 1,705 point elements.
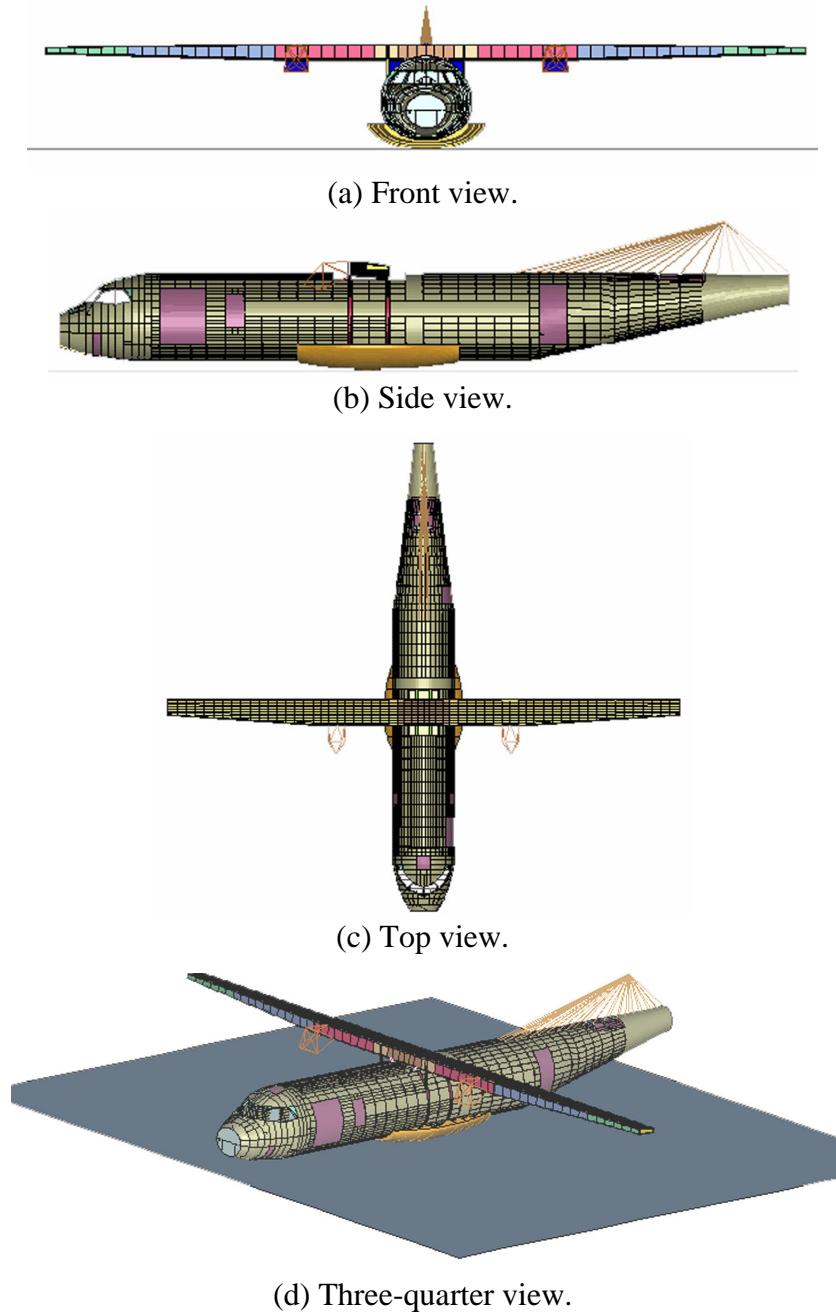
(a) Front view.

(b) Side view.

(c) Top view.

(d) Three-quarter view.

Figure 6. Finite element model of the ATR42 aircraft.

An automatic contact (CONTACT_AUTOMATIC_SINGLE_SURFACE) was specified for the model, which is a generic contact definition in LS-DYNA that prescribes that no node can penetrate through any surface in the model.   An impact surface was created to represent the concrete pad beneath the drop tower. This surface was modeled as a 5-in. thick aluminum plate, encompassing the total length and width of the aircraft, as shown in Figure 6(d). Three main material properties are defined in the model for aluminum Al2024-T3, aluminum Al7075-T6, and titanium Ti-6Al-4V. The properties were defined using the MAT_PLASTIC_KINEMATIC card in LS-DYNA for a linear elastic-plastic material with input values for density, Poisson's ratio, Young's modulus, yield stress, hardening modulus, and an ultimate failure strain. Most of

the sheet metal parts, such as the outer skin were assigned material properties of Al2024-T3. The forged metal parts, such as the fuselage frames, floor beams, and seat tracks were assigned material properties of Al7075-T6.   The "dog bone" specimens used to attach the wing to the fuselage frames at FS 25 and FS 27 were assigned material properties of titanium. The material property designations for each component were obtained from the aircraft manufacturer's Weight and Balance Manual [10] and the material property values were found in MIL-HDBK-5H [11].

The pictures of the model, shown in Figure 6, were obtained from LS-POST [12], the post-processing software for LS-DYNA. A figure depicting the location of the point elements is shown in Figure 7. Point elements were used to assign concentrated masses representing the seats, occupants, luggage, fuel, and other ballast to nodes in the model. The mass distribution of the fuel loading was determined by creating solid elements defined by the upper and lower wing skins, with one element thickness between each skin. The nodes on the bottom skin were fixed. The solid elements were assigned properties with the density of water, and a gravitational loading was applied. The resulting constraint forces on the bottom nodes were converted into a mass loading at each node.   Once this process was complete, the solid elements and nodal constraints were removed.
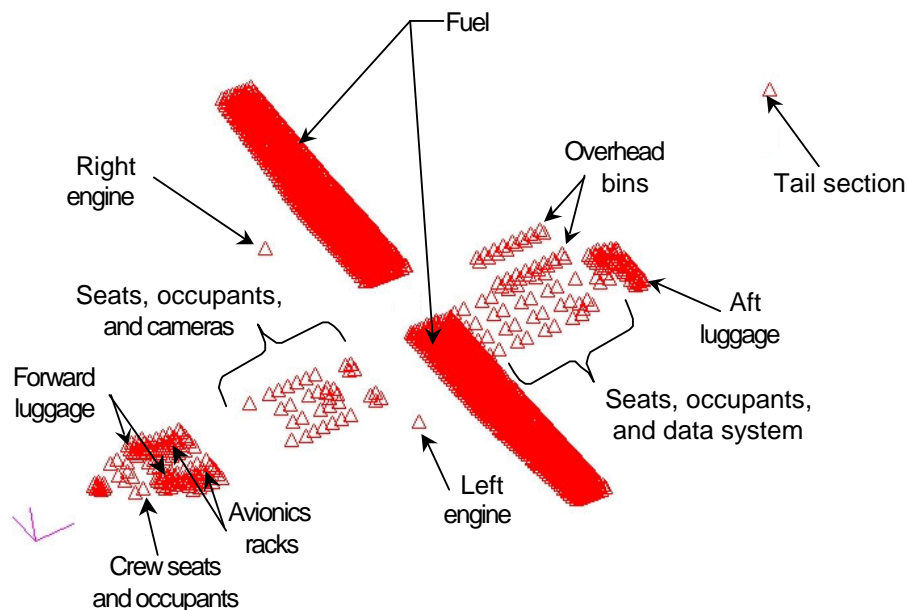

Figure 7. The location of point elements in the model.

All of the nodes in the aircraft model were given an initial velocity of –360 in/s (-30 ft/s). For the impact surface, all of the edge nodes were constrained from translational and rotational motion. The model was executed in LS-DYNA (version 970) for 0.3 seconds of simulation time, which required 130 hours of CPU on a single processor Hewlett Packard workstation x4000.

As a quality check on the model, the total weight and longitudinal CG location of the model were compared with those of the test article. The weight of the aircraft was 33,200 lb. and the total weight of the aircraft model was 32,900 lb., just 300 lb. lighter than the test article.   The measured longitudinal CG position of the test article was 469.2 in. from the reference location. For the model, the longitudinal CG position was 474.1 in. from the reference location, within 5 inches of the experimental value.

Test-Analysis Correlation

The test-analysis correlation consists of comparisons of experimental and predicted structural deformation and selected acceleration and velocity time history responses.

Comparison of Structural Deformation
Comparisons of test article and model deformations are shown in Figure 8 from 0.06- to 0.3-seconds in .06-second intervals. The pictures of model deformation were obtained from the post-processing file, and the experimental pictures were captured from the high-speed film. In general, the model accurately predicts the structural deformation and failure behavior of the test article, including collapse and failure of the fuselage structure beneath the wing. In both the test and analysis, the failure is initiated by fracture of the fuselage frames at FS 25 and FS 27, and not failure of the dog bone specimens. The frame failures allow the wing to translate downward through the fuselage cabin. Some differences between the test and analysis are noted. In the model, the wing exhibits significant flexure, resulting in vertical displacement of the wing tips. This behavior is not seen in the test.
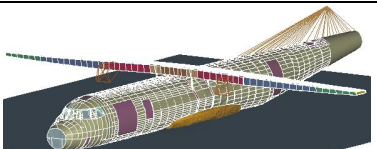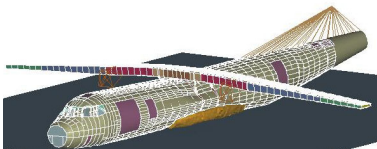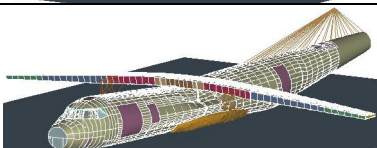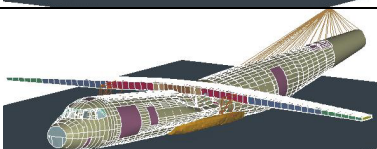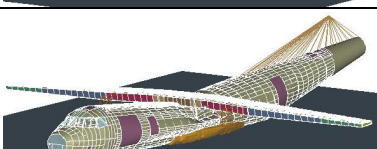
| Time, s	Test article	LS-DYNA simulation
0.06		
0.12		
0.18		
0.24		
0.30		

Figure 8. Comparisons of structural deformation.

Comparison of Selected Acceleration Time History Responses
The raw experimental acceleration data were plotted versus time, integrated to obtain the velocity time history response, and filtered using a low-pass digital filter based on the SAE J211/1 specifications [13]. A variety of cut-off frequencies were applied in an attempt to obtain a discernable single acceleration pulse, while at the same time not distorting the integrated velocity response. The distortion is determined by comparing the velocity responses obtained

by integrating the raw and filtered experimental acceleration data. A filtering frequency of 33.2 Hz was selected because it met these criteria. The experimental and analytical acceleration time histories shown in the paper are filtered at this frequency.

The experimental and analytical acceleration responses of the left outer seat track at FS 20 and the right outer seat track at FS 18 are shown in Figure 9. For the test, the main acceleration pulse is less than 0.1-second in duration, and exhibits two main peaks. For the left outer seat track location, the first acceleration peak is smaller in magnitude than the second, which has a magnitude of 28 g. For the right outer seat track location, the two acceleration peaks are of the same magnitude, about 24 g. In both cases, the predicted acceleration responses also exhibit two peaks, with the second being higher in magnitude than the first. The pulse durations of the analytical responses are almost identical to those of the experimental responses.
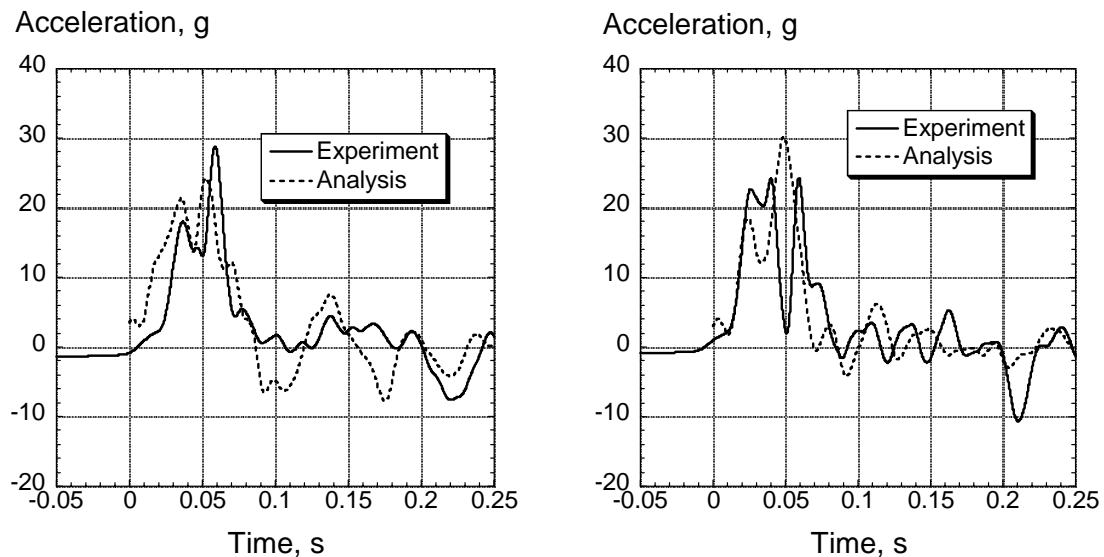
(a) Left outer seat track at FS 20.   (b) Right outer seat track at FS 18.

Figure 9. Experimental and analytical acceleration responses for the left outer seat track at FS 20 and the right outer seat track at FS 18.

The raw experimental and analytical acceleration data were integrated to obtain the velocity responses at these two locations, as shown in Figure 10. For the left outer seat track at FS 20, the experimental and analytical curves are closely matched up to 0.05 seconds. After that time, the analytical velocity response crosses zero velocity at 0.07 seconds and exhibits a rebound of about 60 in/s. Conversely, the experimental response flattens out after 0.05 seconds and does not cross zero until 0.125 seconds. For the right outer seat track at FS 18, the predicted velocity response closely matches the experimental response, i.e. both curves cross zero velocity at the same time (.07 seconds) and both curves exhibit the same rebound velocity of approximately 50 in/s.

Next, the experimental and analytical acceleration responses of the right side of the cockpit floor are plotted in Figure 11. Again, the experimental acceleration response exhibits two peaks; however, in this case the first peak (34 g) is higher in magnitude than the second (28 g). The predicted acceleration response shows a single pulse, of longer duration than the experiment, with a peak acceleration of 32 g.

The experimental and analytical acceleration responses of the left and right inner seat track locations at FS 29 and FS 35, respectively, are plotted in Figure 12. The locations of these two accelerometers are shown in the schematic drawing of Figure 2. The accelerometer at FS 29 is located slightly to the rear of the fuselage frames supporting the wings, while the accelerometer at FS 35 is located at the very rear of the aircraft. The filtered experimental accelerations exhibit high-amplitude, low frequency responses, making it difficult to discern a single acceleration pulse. In general, the predicted acceleration responses show good agreement with the experimental data at these two locations.

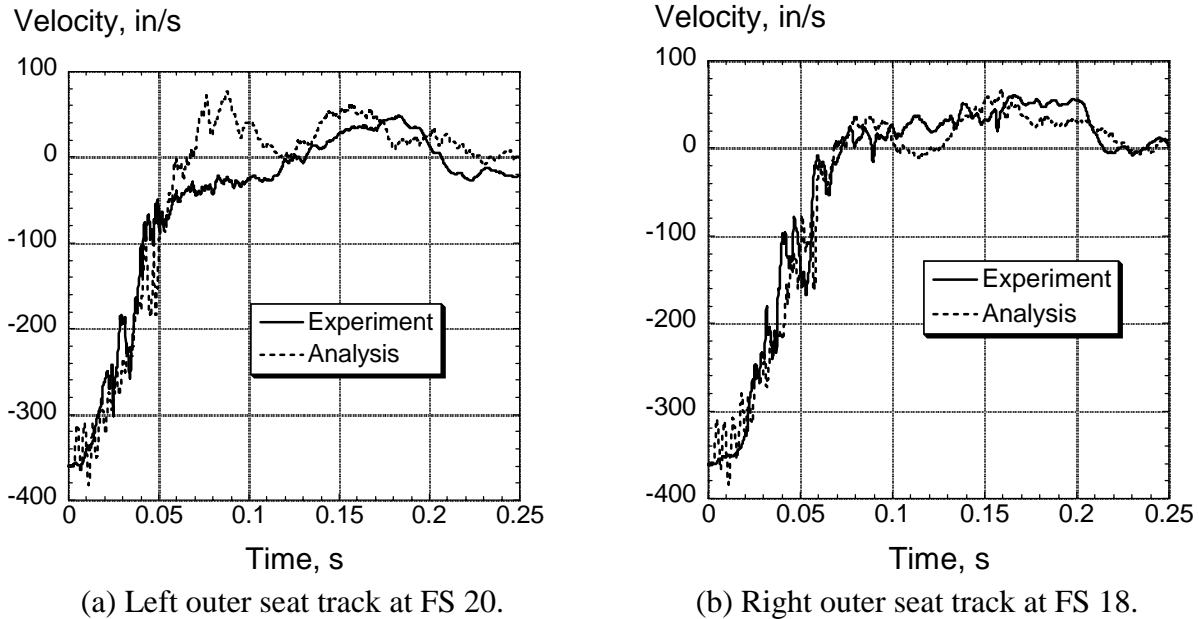(a) Left outer seat track at FS 20.   (b) Right outer seat track at FS 18.

Figure 10. Experimental and analytical velocity responses for the left outer seat track at FS 20 and the right outer seat track at FS 18.
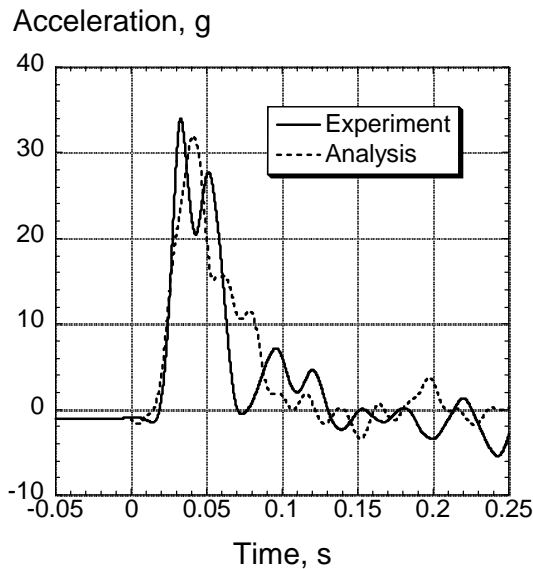
Figure 11. Experimental and analytical acceleration responses of the cockpit floor (right side).

The experimental and predicted acceleration responses of the center of the tail section at FS 47 are plotted in Figure 13. Unlike the floor acceleration responses, which had pulse durations of less than 0.1 second, this response is 0.2 seconds in duration. Both the experimental and analytical acceleration responses exhibit a single pulse, of approximately the same duration, with magnitudes of 12 and 13 g's, respectively.

(a) Left inner seat track at FS 29.   (b) Right inner seat track at FS 35.
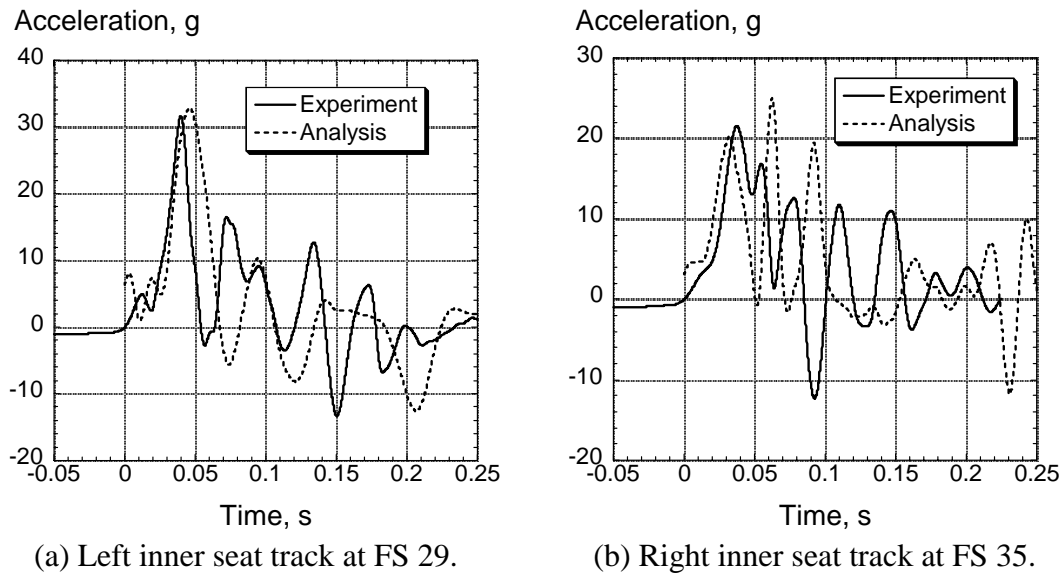
Figure 12. Experimental and analytical acceleration responses of the left and right inner seat track locations at FS 29 and FS 35, respectively.
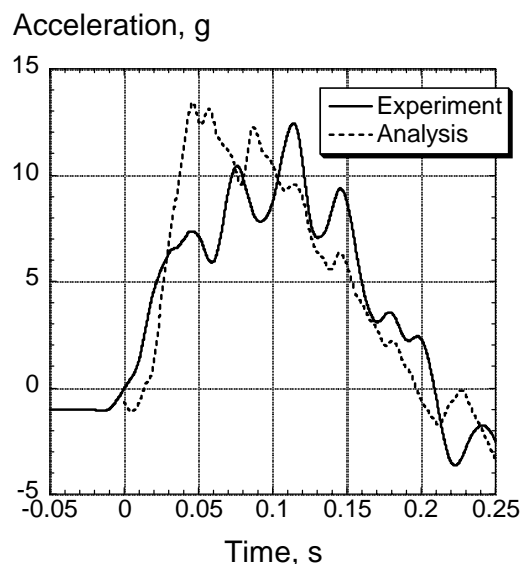

Figure 13. Experimental and analytical acceleration responses of the center of the tail section at FS 47.

The experimental and analytical acceleration responses of the left sidewall at FS 18 are plotted in Figure 14. This accelerometer was located on the sidewall approximately 12 in. above the floor and was oriented in the vertical direction. The analytical acceleration response closely matches

the magnitude (peak acceleration of 25 g's for the analysis compared with 22.5 g's for the experiment) and duration of the experimental pulse.
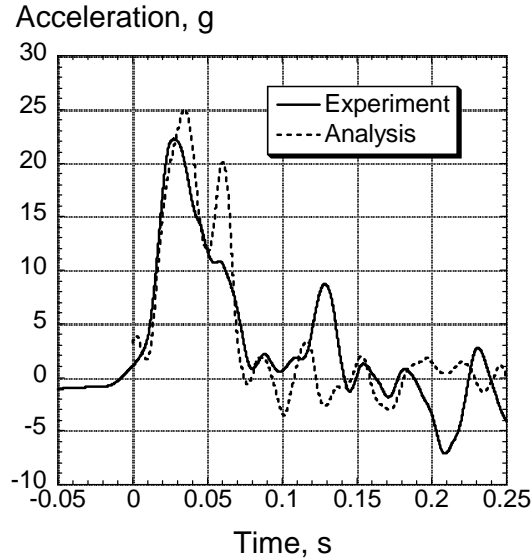
Acceleration, g

Figure 14. Test and analysis acceleration responses of the left sidewall at FS 18.

The final time history comparison is shown in Figure 15, in which the experimental and analytical acceleration responses of the center ceiling at FS 26 are plotted. This location is at the center of the bottom skin of the wing. The filtered experimental and analytical data continue to exhibit high-amplitude, low frequency responses at this location and it is not possible to see a well-defined acceleration pulse. The predicted acceleration response overshoots the magnitude of the initial peak acceleration of the experimental response; however, it accurately captures the dip and subsequent rise in the experimental response that occurs at approximately 0.1 seconds.
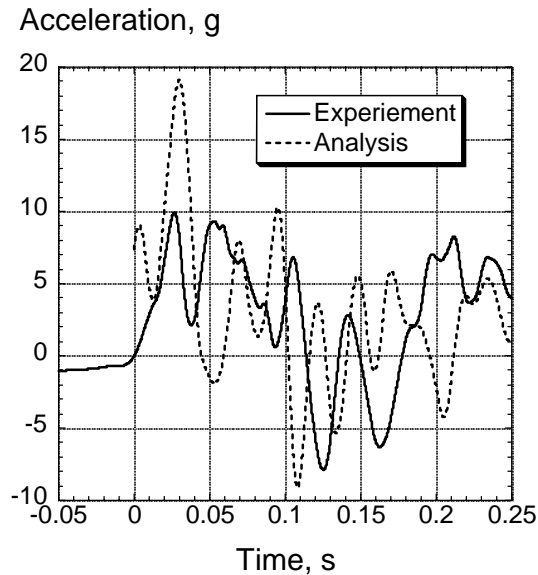
Acceleration, g

Figure 15. Test and analysis acceleration responses of the center ceiling at FS 26.

Discussion of Results

In general, a high level of agreement was obtained between the experimental and analytical data, especially when considering the complexity of the test article and the unsophisticated method of model development. The simulation accurately predicted the major structural failure, the collapse and failure of the fuselage frames supporting the wing structure. However, some differences in the progression of structural damage and deformation were noted. The model exhibited more bending and flexure of the wing than was observed experimentally. This difference in behavior indicates that the material properties and/or average dimensions used in the model should be modified to increase the structural stiffness of the wing.

The model predicted the experimental acceleration time histories quite well. The high level of agreement achieved for the floor-level acceleration responses is important in that these pulses are transmitted to the seats and occupants during a crash. Also, these data are needed to accurately assess dynamic seat criteria for commuter-class aircraft.   It was noted that even after filtering, some of the acceleration responses exhibited high-amplitude, low frequency responses, making it difficult to discern a single acceleration pulse. For other channels, the low-pass filter with a cut-off frequency of 33.2 Hz was able to generate a single acceleration pulse. Thus, for this test, it may be necessary to use different cut-off frequencies when filtering the data, on a channel-by-channel basis. Of course, the analytical data would be filtered at the same frequency as the experimental data at each location.

Concluding Remarks

A full-scale three-dimensional finite element model of a twin-turboprop high-wing commuter-class aircraft, the ATR42-300, was developed and executed as a crash simulation. The analytical predictions were correlated with test data obtained from a 30-ft/s vertical drop test of the aircraft that was conducted using the Dynamic Drop Test Facility at the FAA William J. Hughes Technical Center in Atlantic City, NJ. For the test, the aircraft was configured with seats, anthropomorphic test dummies, luggage in the forward and aft compartments, and 8,700-lb of water in the wings to represent the fuel loading. The finite element model of the aircraft was developed from direct geometric measurements and contained 57,643 nodes and 62,979 elements including 60,197 quadrilateral shell elements; 551 triangular shell elements; 526 beam elements; and, 1,705 point elements.   The model was executed in LS-DYNA, a commercial code for performing explicit transient dynamic simulations.

The analytical predictions correctly simulated the major damage mode seen during the test, which was collapse and failure of the fuselage structure beneath the wing. These structural failures allowed the wing to displace vertically through the fuselage cabin. In general, a high level of agreement was obtained between the experimental and analytical data, especially when considering the complexity of the test article and the unsophisticated method of model development. It was particularly important to obtain accurate prediction of the floor-level acceleration responses, since these pulses are transmitted to the seat and occupants. These data will be useful in evaluating the FAA's proposed dynamic seat standards for commuter-class aircraft.

Acknowledgements

References

1. Noor, A., and Carden H. C., editors, "Computational Methods for Crashworthiness," NASA Conference Publication 3223, October 1993.

2. Abramowitz, A., Smith, T. G, Vu, T., "Vertical Drop Test of a Narrow-Body Transport Section with a Conformable Auxiliary Fuel Tank Onboard." DOT/FAA/AR-00/56, October 2000.

3. Abramowitz, A., Smith, T. G., Vu, T., Zvanya, J. R., "Vertical Drop Test of a Narrow-Body Transport Fuselage Section with Overhead Stowage Bins," DOT/FAA/AR-01/100, September 2002.

4. Anon., "MSC.Dytran User's Manual Version 4.7," The MacNeal-Schwendler Corporation, Los Angeles, CA, 1999.

5. Jackson, K. E. and Fasanella, E. L., "Crash Simulation of a Vertical Drop Test of a B737 Fuselage Section with Overhead Bins and Luggage," Proceedings of the Third Triennial Aircraft Fire and Cabin Safety Conference, Atlantic City, NJ, October 22-25, 2001.

6. Fasanella, E. L. and Jackson, K. E., "Crash Simulation of a Vertical Drop Test of a B737 Fuselage Section with an Auxiliary Fuel Tank," Proceedings of the Third Triennial Aircraft Fire and Cabin Safety Conference, Atlantic City, NJ, October 22-25, 2001.

7. Jackson, Karen E. and Fasanella, E. L., "Crash Simulation of Vertical Drop Tests of Two Boeing 737 Fuselage Sections," DOT/FAA/AR-02/62, August 2002.

8. Anon., "MSC.PATRAN," Publication No. 903077, Version 6, The MacNeal-Schwendler Corporation, 1996.

9. Anon., "LS-DYNA Keyword User's Manual Volume I and II," Livermore Software Technology Company, Livermore, CA, March 2001.

10. Anon., "Weight and Balance Manual," Avions de Transport Regional, Service Bulletin No. ATR42-34-0114, issued March 1992.

11. Military Handbook 5H, U.S. Department of Defense, 1 December 1998.

12. Anon., "LS-PRE/POST v. 1.0 Manual" Livermore Software Technology Company, Livermore, CA, August 27, 2002.

13. Society of Automotive Engineers, Recommended Practice: Instrumentation for Impact Test – Part 1, Electronic Instrumentation, SAE J211/1, March 1995.